

EEG Source Analysis with a Convolutional Neural Network and Finite Element Analysis

Thanos Delatolas¹, Marios Antonakakis¹, Carsten H. Wolters² and Michalis Zervakis¹

Abstract—To reconstruct the electrophysiological activity of brain responses, source analysis is performed through the solution of the forward and inverse problems. The former contains a unique solution while the latter is ill-posed. In this regard, many algorithms have been suggested relying on different prior information for solving the inverse problem. Recently, neural networks have been used to deal with source analysis. However, their underlying training for inverse solutions is based on sub-optimal forward modeling. In this work, we propose a CNN that is able to reconstruct EEG brain activity. To train our proposed CNN, a skull-conductivity calibrated and white matter anisotropic head model. Based on this model, we generate simulated EEG data and used them to train our CNN. We first evaluate the performance of our CNN using the simulated EEG data while a realistic application with somatosensory evoked potentials follows. From the results, we observed that the CCN correctly localized the P20/N20 component at the subject-specific Brodmann area 3b and it can potentially localize deeper sources. A comparison is also presented with well-known inverse solutions (single dipole scans and sLORETA) showing similar localization performance. Through these results, an emerging potential for real applications appears on the basis of realistic head modeling.

I. INTRODUCTION

To perform Electroencephalography (EEG) or Magnetoencephalography (MEG) source analysis, we need to solve the forward problem which relies on the flow-estimation of the electric field to the EEG or MEG sensors for a given brain source. The next problem is the estimation of an inverse solution for which we reconstruct the neuronal activity given the original EEG or MEG data and the forward solution on the basis of a three-dimensional geometry of the head.

The EEG/MEG forward solution has been proved to be unique [3]. The most commonly used numerical techniques that solve the forward problem are the Bounded Element Method (BEM) [4] and Finite Element Method (FEM) [5]. In this study, we opted for FEM because of its high flexibility to accurately model the electromagnetic field propagation in geometrically challenging inhomogeneous and anisotropic head volume conductors such as the human head [3].

¹Thanos Delatolas, Marios Antonakakis and Michalis Zervakis are with the School of Electrical and Computer Engineering, Technical University of Crete, 73100 Chania, Crete, Hellas (phone: +30-28210-37216; e-mail: {adelatolas, mantonakakis, mzervakis}@tuc.gr)

²Carsten H. Wolters is with the Institute for Biomagnetism and Biosignalanalysis, Otto Creutzfeldt Center for Cognitive and Behavioral Neuroscience, University of Munster, Munster, Germany (carsten.wolters@uni-muenster.de)

*Research supported partly by the European Union and Greek national funds through the EPAnEK (projects: SmartHealth (Type of action: DIGITAL-SIMPLE, grant no. 101083630), x (epi)VLEPSIS (T1EDK-04440))

During the inverse solution, an endless number of source and parameter configurations can yield the same EEG/MEG measurements, characterizing the EEG/MEG inverse problem as ill-posed [2]. A wide range of inverse reconstructions based on various a priori assumptions have been created. These reconstructions are broadly classified as an equivalent current dipole, current density reconstruction, beamforming, and hierarchical Bayesian modeling [3]. In this work, Single Dipole Scan [14] and sLORETA [15] are used for source localization evaluations in additionally to our proposed solution.

These two source localization techniques have been evaluated [2], but prior knowledge is important making the problem laborious and posing also problems for real-time applications. Recently, Deep Learning methods have been proposed to overcome these limitations. A Multi-Layer Perceptron (MLP) network [9] and various CNNs such as [7], [8]. Deep Learning has the potential to offer real-time source localization. However, in these methods, no accurate and realistic head modeling is used which can potentially lead to suboptimal source reconstructions.

In this work, we propose a new finite-element-based CNN architecture for source reconstruction of somatosensory evoked potentials. We first create a number of simulated brain source signals using an individually skull-conductivity calibrated and white-matter conductivity anisotropic head model. For the specific head model, finite elements (geometrically adapted hexahedrons) are used. We then train our proposed CNN with input of the scalp topographies of the simulated data and evaluate its performance with the localization error for different levels of noise. Finally, we test our trained model with real somatosensory evoked responses for the localization of the P20/N20 component.

II. METHODS

A. EEG forward problem

The forward problem is concerned with the computation of the channels measurements $\mathbf{M} \in \mathbb{R}^N$ given the moments (magnitude and orientation) $\mathbf{D} \in \mathbb{R}^p$ of the dipoles. Thus, it can be expressed mathematically over time as [2]:

$$\mathbf{M} = \mathbf{G}\mathbf{D} + \mathbf{n} \quad (1)$$

where $\mathbf{M} \in \mathbb{R}^{N \times t}$, $\mathbf{G} \in \mathbb{R}^{N \times p}$ is the leadfield matrix which describes the flow of electrical current of each dipole through every electrode, $\mathbf{D} \in \mathbb{R}^{p \times t}$, and \mathbf{n} is the noise of the recording system.

Moreover, the EEG electrodes are located on the scalp while the dipoles are inside the head. Therefore, a head

model is required which is a simulation of the geometrical and electromagnetic features of the head. We utilized a six-compartment head model [1]. The compartments and their isotropic conductivities are skin $0.43 S/m$, skull compacta $0.31 S/m$, skull spongiosa $0.01116 S/m$, cerebrospinal fluid (CSF) $1.79 S/m$, white and gray matter. The anisotropic conductivity tensors for the compartments of gray and white matter were determined in [1].

Based on the above-mentioned head model, a source space with 50460 dipoles was created in [1]. The dipoles were placed 2 mm far away from the neighbor compartment (i.e., skull compacta or CSF) to fulfill the so-called ‘‘St. Venant’’ condition [1]. Because our neural network could not converge with this extremely detailed source space, we down-sampled it to $p = 10,092$ dipoles. A source space with 10,092 sources is still more accurate than the ones that have been used in the latest Deep Learning studies [7], [8], [9]. Moreover, we used an EEG recording system with $N = 74$ electrodes.

Finally, we utilized DUNEuro [6] in order to calculate the leadfield matrix and thereby solve the forward problem with the Finite Element Method (FEM).

B. Simulation of EEG snapshots

Having solved the forward problem, we can now proceed to the solution of the inverse problem, that is, to estimate the most possible source activity which could generate the scalp EEG recordings. Since the inverse problem is solved using a neural network, we must generate the training dataset. To train a deep learning model and evaluate its performance, we need to know the exact location and moment of the underlying neural sources that give rise to the EEG data.

Our neural network is designed to operate on single-time instances of EEG data with a single source. Thus, we simulate the electrical activity as described in [7]. In particular, each simulation had one dipole cluster, which can be thought of as a smooth area of brain activity. A dipole cluster was created by randomly selecting a dipole in the source space and then applying a region-growing approach. Starting from a single seeding dipole, we recursively incorporated all surrounding neighbors, resulting in a bigger source extent with each iteration. The seed dipole was assigned to an amplitude between 5 and 10 Nano-Ampere Meters (nAm). The amplitude of adjacent dipoles was attenuated based on their distance from the seed dipole. The attenuation followed a Gaussian distribution $\mathcal{N}(0, \frac{\text{distance_from_seed}}{2})$.

The simulated electric activation $\mathbf{D} \in \mathbb{R}^p$ of $p = 10,092$ dipoles was then projected to the leadfield matrix $\mathbf{G} \in \mathbb{R}^{N \times p}$ in order to calculate the potentials at the 74 EEG electrodes $\mathbf{M} \in \mathbb{R}^N$ placed on the scalp. We now differ from the approach of [7] and simulate the potentials of the EEG-electrodes with the following procedure. To generate realistic training data, we added Gaussian white noise at a specific signal-to-noise ratio (SNR) level. The SNR is set based on the power of the neural sources to be 15 dB:

$$\text{SNR} = 10 \cdot \log \left(\frac{P_{\text{signal}}}{P_{\text{noise}}} \right) \quad (2)$$

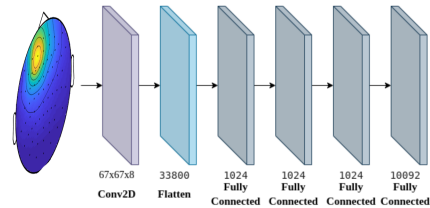


Fig. 1: Proposed CNN

where P_{signal} is the power of the simulated electric activation and P_{noise} is the power of the additive Gaussian noise (unknown variable in the above equation). Finally, from the simulated 74 channel measurements we create their topography using FieldTrip [10]. With the aforementioned algorithm, a set of 100,000 training samples (electrical currents of neural sources and their respective topographies) were produced. Since each simulation contained one dipole cluster, we produce single source EEG snapshots.

C. The finite-element-based CNN for EEG inverse source reconstructions

The design and training of the proposed CNN (see Fig. 1) was accomplished using the Tensorflow [11] and Keras [12] libraries. The proposed network takes as input an EEG topography and predicts the electrical current of each dipole in the source space. Thus, our CNN can be mathematically described as:

$$\Phi : \mathbb{R}^{67 \times 67} \longrightarrow \mathbb{R}^{10092} \quad (3)$$

The input topography passes through a two-dimensional (2D)-Convolution layer with 8 filters that have a size of 2×2 . Furthermore, the output tensor $\mathbf{g} \in \mathbb{R}^{65 \times 65 \times 8}$ is flattened in order to traverse three fully connected layers with 1024 neurons each. Before each one of these three layers, there are also Batch Normalization [13] and Dropout [13] layers. Finally, each neuron of the output layer corresponds to a dipole in the source space and as a result, our CNN predicts the amplitude of each dipole.

We experimented with several loss functions for regression problems but we ultimately decided to use the Mean absolute error (MAE) (4) as it allowed a fast convergence of our CNN compared to others. If \mathbf{y} denotes the true values, $\tilde{\mathbf{y}}$ the predicted values, and N the length of both the vectors with actual and predicted values, MAE can be mathematically described as [13]:

$$L(\mathbf{y}, \tilde{\mathbf{y}}) = \frac{1}{N} \sum_{i=1}^N |y_i - \tilde{y}_i| \quad (4)$$

Moreover, we opted for Rectified Linear Unit (ReLU) [13] it has demonstrated superior performance in tests when compared to alternative activation functions.

Finally, convolution filters, weights, and biases were optimized using the Stochastic Gradient Descent (SGD) algorithm [13] with a learning rate $\lambda = 0.001$ and batch size of 32. The proposed convolutional neural network was

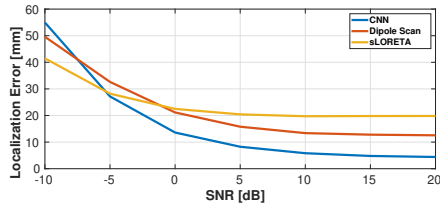


Fig. 2: Localization Error for various SNR levels

trained with 100,000 simulated sources and their respective topographies over 500 epochs in the Jetson AGX.

III. EVALUATION

We now evaluate the performance of our CNN and compare it to state-of-the-art inverse algorithms, namely sLORETA [15] and Single Dipole Scan [14]. We assessed the performance of the neural network using both simulated and real EEG recordings. The localization error (LE) [16] is used as a metric to quantify EEG source localization performance. LE can be quantified as the Euclidean distance between truly activated source r_{true} and the reconstructed peak source r_{peak} in three-dimensional source space:

$$\text{LE} = \|r_{\text{true}} - r_{\text{peak}}\|_2 \quad (5)$$

A. Evaluation for various SNR levels

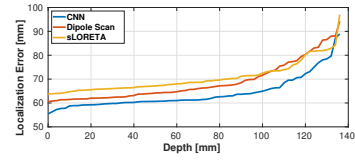
We ran simulations with various SNR levels to measure localization accuracy in several actual conditions. While our CNN is trained with 15 dB SNR data, we used SNR levels ranging from -10 dB to 20 dB in the evaluation. For each SNR level, 5,000 samples (EEG and sources data) were simulated. The localization error for each SNR level is shown in Fig. 2. Our CNN outperformed traditional methods at high SNR levels but performed worse at low SNR levels (< -7.5 dB).

B. Influence of the depth of the simulated source

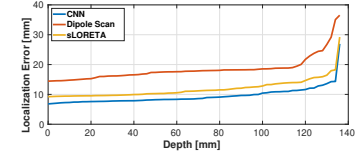
The effect of the source's depth is investigated. The larger the depth of the seed dipole, the less it influences the EEG signal which results in more difficult localization. We compared the performance of the inverse methods for all the depths in the source space and different SNR levels (see Fig. 3). Another finding is that our CNN is capable to correctly localizing even deep sources. In particular, while Dipole Scan has the worst localization results and strongly depends on the depth of the source, both our CNN and sLORETA slightly depend on the depth of the source cluster. Furthermore, for all Signal-to-noise ratios, our CNN yields less localization error over the spectrum of the depths. Finally, as expected, as the SNR increases the dependence of the localization methods on the depth of the neural source decrease and thereby they yield better results.

C. Evaluation with real data

To realistically evaluate the performance of the inverse methods, we used real EEG recordings. They are adapted from [1] and they can be found here [17]. As described

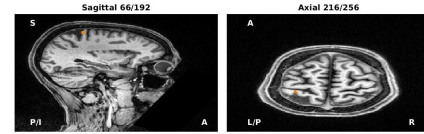


(a) SNR = -10 dB

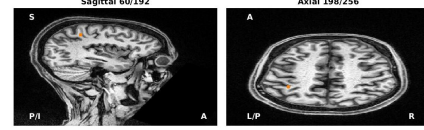


(b) SNR = 10dB

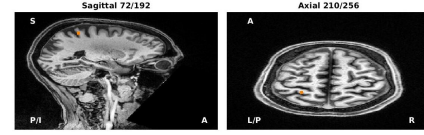
Fig. 3: Localization Error for various SNR levels and depths



(a) Our CNN



(b) sLORETA



(c) Dipole Scan

Fig. 4: Source Localization with real EEG data

in [1], Somatosensory evoked potentials (SEP) were acquired using 80 AgCl sintered ring electrodes (EASYCAP GmbH, Herrsching, Germany, 74 EEG channels plus additional six channels to detect eye movements). The median nerve at the right wrist of five right-handed healthy subjects was stimulated with monophasic square-wave electrical pulses having a duration of 0.5 ms.

Having preprocessed with FieldTrip [10] the Somatosensory evoked potentials, we localized them with all the inverse methods. The localizations projected on the MRI of the subject are shown in Fig. 4.

Principally, in real EEG recordings, as opposed to simulated ones, we cannot know the location of the dipole cluster that gave rise to the recorded EEG signal. Therefore, we cannot use the localization error to quantify the performance of the inverse methods. However, the EEG recordings were generated by a very specific experiment with particular parameters, and many studies [18], [19] verify that this type of stimulus is localized in the Primary Somatosensory Cortex (S1).

It can be seen from Fig. 4 that both our neural network and Dipole Scan correctly localize the SEP to the S1, while

sLORETA estimates inaccurately a deeper location.

IV. DISCUSSION & FUTURE DIRECTIONS

In this study, we propose a CNN for EEG source localization. Initially, to model realistically the geometrical and electromagnetic features of the head, we solve the forward problem using a six-compartment head model based on [1]. Having calculated the leadfield matrix, we simulate EEG recordings and their respective electric activations in the source space. Moreover, we train our model using the electric activations as target data and their corresponding topographies as input. Finally, we assess the accuracy and robustness of the proposed network with both real and simulated EEG data.

Within the limited scope of our experiments, our approach seems to compare very favorably to well-known inverse methods. The results in the simulated data suggest that our model appears reasonable localizations compared to sLORETA and dipole scans. Even though our CNN is trained with 15 dB SNR data, it can correctly localize EEG data in a wide range of SNR levels (see Fig. 2). Moreover, by comparison with the sLORETA and Single Dipole Scan methods, is less dependent and almost independent (for high SNR levels) on the source depth (see Fig. 3). Eventually, our CNN has the generalization ability to correctly localize the somatosensory evoked potentials to S1 (see Fig. 4).

However, our method despite the advantages comes with limitations. First of all, the orientations of the dipoles in the head model are not estimated. Furthermore, our approach is under the assumption that brain activity is always smooth. As a future solution is to generate a proportion of the training data with Random Markov Fields while the rest of them could follow a Gaussian distribution. Moreover, our model is not trained to localize EEG data in a distributed dipole model with more than one source. We intend to expand our method in order to resolve this issue if each simulation contains more than one dipole cluster. Also, our method was only applied to physiological data (i.e. SEP) and still, the localization performance on pathological activity towards an automotive biomarker [21] is questionable. Thus, in the near future, we intend to evaluate the network with pathological brain activity. Finally, our method is not independent of the source space and the anatomy of the brain as it is under the assumption that all source spaces have 10,092 dipoles.

We now compare our model with ConvDip [7], ESNB [9] and DeepMeg [8] in terms of forward modeling and architecture. ConvDip [7] and ESNB [9] use relatively small source spaces with 5124 and 1024 dipoles respectively, while our model and DeepMeg [8] have learned to localize data in 10092 and 15002 dipoles respectively. Moreover, our model and ESNB [9] solved the forward problem using FEM, whereas ConvDip [7] using BEM and DeepMeg [8] using BrainStorm [20]. All neural networks, except DeepMeg [8] which predicts the location(s) of the electric activation(s), estimate the amplitude of each dipole. Furthermore, DeepMeg [8] and ESNB [9] take as input the channel measurements while our CNN and ConvDip [7] take the

topography generated from the EEG electrodes. Finally, our CNN, ConvDip [7] and ESNB [9] have correctly localized real EEG recordings.

We showed that our CNN is capable to localize EEG recordings in a realistic anatomy. Thus, our CNN is a promising inverse solver and with enough future expansions, it could potentially pave the way for real-time source localization.

REFERENCES

- [1] M. Antonakakis et al., "The effect of stimulation type, head modeling, and combined EEG and MEG on the source reconstruction of the somatosensory P20/N20 component," *Hum. Brain Mapp.*, vol. 40, no. 17, pp. 5011–5028, 2019.
- [2] R. Grech et al., "Review on solving the inverse problem in EEG source analysis," *J. Neuroeng. Rehabil.*, vol. 5, no. 1, p. 25, 2008.
- [3] M. Antonakakis, "The effect of experimental and modeling parameters on combined EEG/MEG source analysis and transcranial electric stimulation optimization of somatosensory and epilepsy activity," University of Münster, Münster, 2021.
- [4] J. C. de Munck, C. H. Wolters, and M. Clerc, "EEG and MEG: forward modeling," in *Handbook of Neural Activity Measurement*, R. Brette and A. Destexhe, Eds. Cambridge: Cambridge University Press, 2012, pp. 192–256.
- [5] C. H. Wolters, A. Anwander, G. Berti, and U. Hartmann, "Geometry-adapted hexahedral meshes improve accuracy of finite-element-method-based EEG source analysis," *IEEE Trans. Biomed. Eng.*, vol. 54, no. 8, pp. 1446–1453, 2007.
- [6] S. Schrader et al., "DUNEuro-A software toolbox for forward modeling in bioelectromagnetism," *PLoS One*, vol. 16, no. 6, p. e0252431, 2021.
- [7] L. Hecker, R. Rupperecht, L. Tebartz Van Elst, and J. Kornmeier, "ConvDip: A convolutional neural network for better EEG source imaging," *Front. Neurosci.*, vol. 15, p. 569918, 2021.
- [8] D. Pantazis and A. Adler, "MEG source localization via deep learning," *arXiv [eess.SP]*, 2020.
- [9] C. Wei, K. Lou, Z. Wang, M. Zhao, D. Mantini, and Q. Liu, "Edge sparse basis network: A deep learning framework for EEG source localization," in *2021 International Joint Conference on Neural Networks (IJCNN)*, 2021.
- [10] R. Oostenveld, P. Fries, E. Maris, and J.-M. Schoffelen, "FieldTrip: Open source software for advanced analysis of MEG, EEG, and invasive electrophysiological data," *Comput. Intell. Neurosci.*, vol. 2011, p. 156869, 2011.
- [11] Martín Abadi et al., *Tensorflow: A system for large-scale machine learning*, 2015.
- [12] F. Chollet, Keras. 2015.
- [13] I. Goodfellow, Y. Bengio, and A. Courville, *Deep Learning*. London, England: MIT Press, 2016.
- [14] M. Fuchs et al., "Improving source reconstructions by combining bioelectric and biomagnetic data," *Electroencephalogr. Clin. Neurophysiol.*, vol. 107, no. 2, pp. 93–111, 1998.
- [15] R. D. Pascual-Marqui, "Standardized low resolution brain electromagnetic tomography (sLORETA): Technical details" in *Methods and findings in experimental and clinical pharmacology*, pp. 5–12, 02 2002.
- [16] F. Lucka, S. Pursiainen, M. Burger, and C. H. Wolters, "Hierarchical Bayesian inference for the EEG inverse problem using realistic FE head models: depth localization and source separation for focal primary currents," *NeuroImage*, pp. 1364–1382, 2012.
- [17] M. C. PIASTRA et al., "The WWU DUNEuro reference data set for combined EEG/MEG source analysis." 2020.
- [18] A. Nakamura et al., "Somatosensory homunculus as drawn by MEG," *Neuroimage*, vol. 7, no. 4 Pt 1, pp. 377–386, 1998.
- [19] D. van Westen, P. Fransson, J. Olsrud, B. Rosén, G. Lundborg, and E.-M. Larsson, "Fingersomatopy in area 3b: an fMRI-study," *BMC Neurosci.*, vol. 5, p. 28, 2004.
- [20] F. Tadel, S. Baillet, J. C. Mosher, D. Pantazis, and R. M. Leahy, "Brainstorm: a user-friendly application for MEG/EEG analysis" *Computational intelligence and neuroscience*, 2011.
- [21] V. Sakkalis "Applied strategies towards EEG/MEG biomarker identification in clinical and cognitive research" *Biomarkers in medicine* 5 (1), 93-105